Macromolecular Materials and Engineering

Macromolecular Materials and Engineering Open Access

www.mame-journal.de

RESEARCH ARTICLE OPEN ACCESS

Optimizing Mechanical and Electrical Performance in EPDM Composites for Spacer Dampers: A Balanced Approach via Carbon Black Ratio and Protective Waxes

Masoud Tayefi[1] | Mostafa Eesaee[1] | Meysam Hassanipour[2] | Said Elkoun[3] | Eric David[4] | Phuong Nguyen-Tri[1]

[1]Laboratory of Advanced Materials For Energy and Environment (Nguyen-Tri lab), Université du Québec à Trois-Rivières (UQTR), Trois-Rivières, Québec, Canada | [2]Hydro-Québec Research Center, Varennes, Québec, Canada | [3]Center For Innovation in Technological Eco-Design (CITE), University of Sherbrooke, Sherbrooke, Québec, Canada | [4]Mechanical Engineering Department, École de Technologie Supérieure (ETS), Montréal, Québec, Canada

Correspondence: Phuong Nguyen-Tri (phuong.nguyen-tri@uqtr.ca)

Received: 6 November 2025 | **Revised:** 23 December 2025 | **Accepted:** 7 January 2026

Keywords: carbon black | electrical conductivity | electrical overhead lines | EPDM rubber | mechanical properties | wax

ABSTRACT

Electrical overhead lines rely on spacer dampers to prevent bundled conductors from colliding during wind and ice events, but these devices often suffer from performance loss, displacement, mechanical failure, and material degradation over time. Since installation and replacement are dangerous, slow, and costly, improving the materials and design of spacer dampers is essential for long-term reliability. As it was studied in the previous article, the actual elastomer is sensitive to aging. Therefore, in this study, it was explored how different types of ethylene propylene diene monomer (EPDM), carbon black (CB), and waxes affect the properties of elastomeric composites. The results of the tensile test of three types of EPDM showed that the one with the highest ethylene content had the highest stress and elongation at break. The experiment changed the ratio of two types of furnace carbon black through a series of mechanical, electrical, and physical tests. It represented that increasing the amount of carbon black with a smaller size and higher surface area (N330) improved the stress and elongation at break of EPDM composites, but made it less conductive. For the swelling test, also observed that the insoluble fraction was the same for all samples; however, samples with more N330 tended to swell more, indicating a lower crosslink density. Additionally, examining the effects of five types of waxes on the mechanical properties showed that a balanced property can be obtained by adding the blend of microcrystalline and paraffin wax, in which elongation at break and 100% modulus increased slightly, and stress at break decreased marginally in comparison to that of the control sample. Upon aging, the blend of two waxes had much retention of stress and elongation at break upon aging which means that it was more effective in protecting materials.

1 | Introduction

Electrical overhead transmission lines are crucial for transferring electricity from power plants to consumers. A major concern arises when bundled conductors collide due to strong winds or ice build-up, which can lead to destructive conditions for the lines [1–3]. The most common and effective solution is the use of a spacer damper, which maintains the proper distance between conductors and helps mitigate wind-induced vibrations. However, over time, these spacers can experience issues such as malfunction, displacement, structural breakage, and material degradation [3–6]. Furthermore, the installation and replacement of these spacers are inherently difficult, dangerous, slow, and costly due to their location high on the lines [6, 7]. Consequently, the materials and methods used in the production of these spacer dampers require thorough study and improvement.

TABLE 1 | The specifications of the EPDMs, CBs, and the waxes.

The specifications of the EPDMs		
Trade name	**Ethylene content (wt.%)**	**Abbreviation used in the article**
Keltan 2470	69	E47
Keltan 2450	48	E45
Keltan 2650	53	E65

The specifications of the CBs				
	Surface Area (m^2/g)[a]	**BET Surface Area (m^2/g)[b]**	**Sulfur (wt.%)[a]**	**Abbreviation used in the article**
5345R	36.3	39.5	1.26	N550
5358R	79.0	81.0	0.26	N330

The properties of the five types of waxes			
	Melting point (°C)	**Type**	**Abbreviation used in the article**
BW-408[a]	62.8	Microcrystalline Wax	MC-408
BW-431[a]	82.2		MC-431
BW-433[a]	48.9	Paraffin Wax	PW-433
BW-436[a]	65.6		PW-436
Nochek 4756A[b]	63–66	Microcrystalline/paraffin wax blend	Blend

[a]Produced by Blended Waxes Inc., USA.
[b]Produced by Sovereign Chemical Company, USA.

The saturated backbone of ethylene propylene diene monomer (EPDM), characterized by a lack of double bonds, confers exceptional resistance to degradation from oxygen, UV radiation, and ozone. Consequently, this elastomer is widely utilized for critical applications such as wire insulation and weather sealing [8, 9]. regarding reinforcement, carbon black (CB) is a pivotal additive in the rubber industry; it significantly enhances mechanical performance while simultaneously increasing electrical and thermal conductivity [10–12]. Research has extensively focused on EPDM composites reinforced with carbon black. For instance, increasing the loading of N330 CB has been shown to substantially improve tensile and compression properties relative to unfilled EPDM [13]. Similarly, studies on peroxide-cured EPDM composites for fuel cell gaskets observed that higher CB content resulted in increased electrical conductivity, tensile stress, modulus, and hardness. However, this reinforcement came at the cost of an increased compression set, highlighting the necessity of optimizing the formulation to balance conflicting performance requirements [14].

A recent comparative study of Printex and HAF CBs in peroxide-cured EPDM composites revealed that the Printex-filled material exhibited superior tensile stress, modulus, dielectric constant, and electromagnetic interference (EMI) shielding [11]. Regarding the mechanism of peroxide curing, it was observed that the specific surface area and sulfur content of the carbon black are critical factors. Specifically, carbon blacks with higher surface area and sulfur content facilitate the formation of physical and chemical crosslinks, respectively. This results in increased hardness, modulus, and tensile strength, but reduced elongation at break [15]. In another study aiming to develop overhead line wire clamps with high thermal aging resistance and grip, EPDM utilizing a hybrid peroxide and sulfur cure system was reinforced with varying carbon blacks and glass flakes. Evaluations of three CB grades (N330, N539, and N774) indicated that N330 provided semi-conductivity and high tensile strength, whereas N774 offered superior resistance to compression set and heat aging, with N539 displaying intermediate properties. Optimization of the N330:N774 ratio revealed that a 50:20 blend achieved the desired balance of semi-conductivity, mechanical strength, and aging resistance. Furthermore, the incorporation of glass flakes increased the grip force of the clamp by a factor of 1.8 compared to the unmodified rubber [16].

A study investigating the influence of three types of plasticizers (liquid butadiene, polyethylene wax, and paraffinic oil) on highly filled, peroxide-cured EPDM revealed that liquid butadiene caused the most significant reduction in crosslink density, followed by polyethylene wax and paraffinic oil. Generally, the addition of these softeners resulted in a decrease in tensile stress and an increase in elongation at break. Upon thermal aging at 150°C, the stress at break decreased, while the elongation at break showed a slight increase. These results were attributed to the formation of a network of small crosslinks during aging, initiated by residual peroxide or polymer radicals within the softener phase; consequently, this mechanism altered the stress at break without significantly changing the overall chemical crosslink density [17]. In our previous works, we reviewed the aging behavior of elastomers and the methodologies used to estimate their lifetime [18–20]. This foundation enabled us to assess industrial products in terms of their efficiency and durability, as

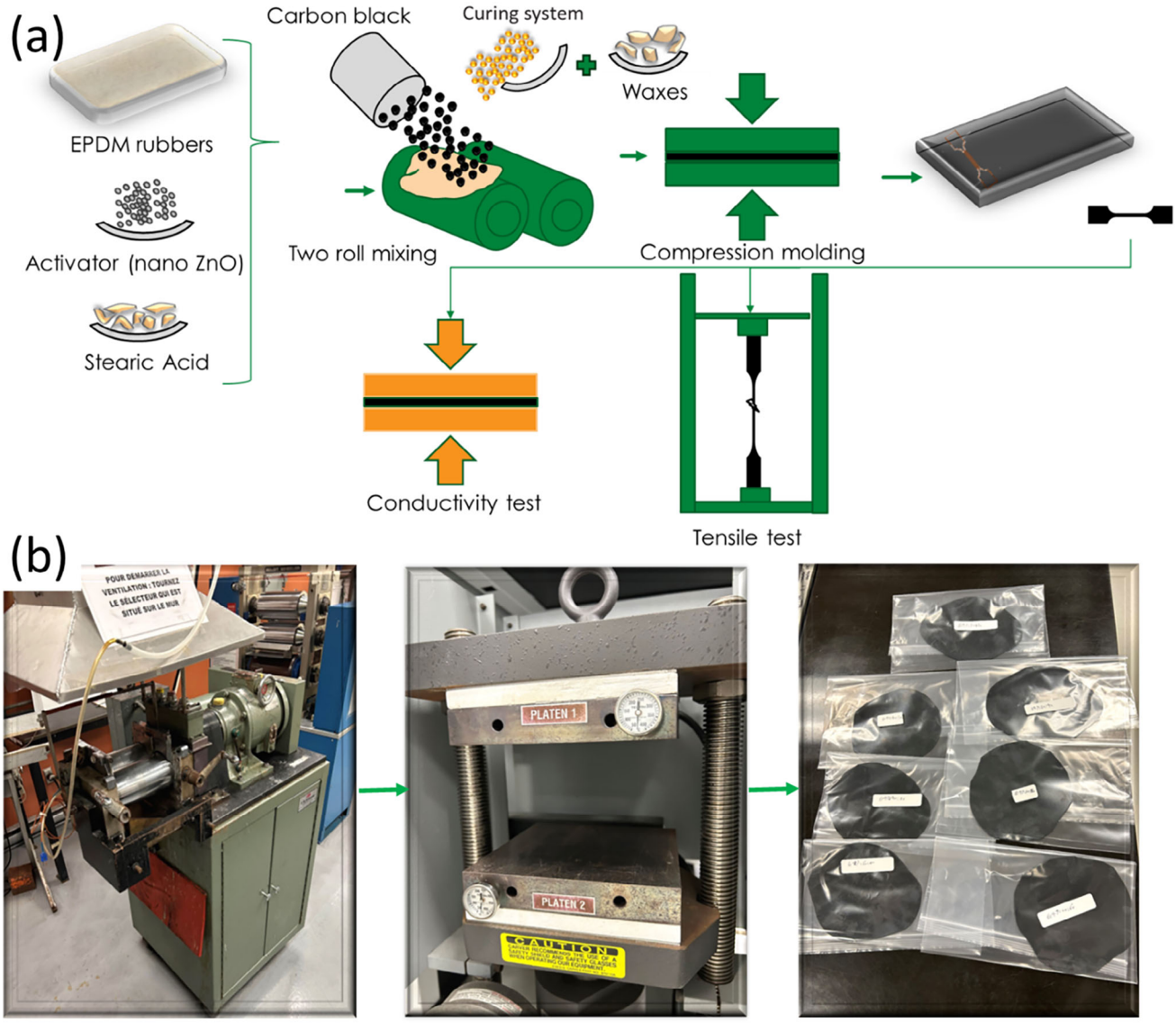

FIGURE 1 | (a) The schematic of methodology for preparing and testing the samples, (b) The images of the used equipment and the prepared samples.

recently published [21, 22]. These recent findings have provided deeper insight into how such products can be reformulated to develop more efficient alternatives.

Although the influence of carbon black structure, crosslink density, and protective additives on EPDM properties has been individually addressed in the literature, the combined effects of these components within the same formulation remain insufficiently explored. In particular, there is a lack of studies that simultaneously consider mechanical reinforcement, electrical conductivity, and thermo-oxidative aging resistance, which are essential performance criteria for high-voltage spacer damper applications. Moreover, most previous works have relied on academic formulations, providing limited insight into the behavior of the CB and wax commercial grades under realistic performance requirements. Therefore, this study aims to fill this gap by systematically investigating how the two types of carbon black structures, their combinations, and different waxes influence the electrical, mechanical, and aging behavior of EPDM compounds specifically designed for vibration-damping components in overhead transmission lines.

In this study three commercial grades of sulfur-cured EPDM were initially evaluated to identify the optimal base elastomer. Subsequently, the formulation was reinforced using carbon blacks with distinct surface areas, structures, and particle sizes to meet the specific conductivity and mechanical standards of the application. To optimize these properties, a systematic investigation was conducted on the effects of varying the ratios of two carbon black types (N330 and N550) on the composite's electrical and mechanical behavior. Furthermore, the crosslink density and swelling behavior were analyzed to elucidate the interaction between the fillers and the rubber matrix. Finally, to address the long-term durability requirements against environmental factors, the protective efficacy of various wax systems was assessed. The impact of these additives on the retention of mechanical properties after thermo-oxidative aging was examined to determine the most effective formulation strategy for this critical application.

TABLE 2 | The formulations to compare the types of EPDM.

Name E(type):C330:C550	Rubber(phr)	CB 330(phr)	CB 550(phr)	Wax (Phr)
E45:00:00	100	00	00	0
E65:00:00	100	00	00	0
E47:00:00	100	00	00	0
E45:30:30	100	30	30	0
E47:30:30	100	30	30	0
E47:00:60	100	00	60	0
E47:10:50	100	10	50	0
E47:20:40	100	20	40	0
E47:30:30	100	30	30	0
E47:40:20	100	40	20	0
E47:50:10	100	50	10	0
E47:60:00	100	60	00	0
E47:30:30:MC-408	100	30	30	1 (MC-408)
E47:30:30:MC-431	100	30	30	1 (MC-431)
E47:30:30:PW-433	100	30	30	1 (PW-433)
E47:30:30:PW-436	100	30	30	1 (PW-436)
E47:30:30:Blend	100	30	30	1 (Blend)

2 | Materials and Methods

2.1 | Materials

Three types of EPDM with the trade names of Keltan 2470, Keltan 2450, and Keltan 2650 were procured from Arlanxeo. Other components were two grades of CB, which were N550 and N330 were procured from Asbury Carbons, USA. Five types of waxes were also used in the work. The information on EPDMs, CBs, and waxes has been tabulated in Table 1. An industrial-grade sulfur curing system was used for the curing of elastomers.

2.2 | Formulations and Mixing

The rubber compounding was carried out on a laboratory open two-roll mill (Brabender, USA) with a friction ratio of 1:1.2. The rolls were equipped with internal water circulation to maintain the temperature at approximately 25–30°C and prevent scorching. The roll speed was maintained at approximately 48 rpm. The mixing procedure was consistent for all samples. First, the EPDM rubber was masticated on the mill for 2 min to create a smooth band. The activators were then added and mixed for 15 min. Subsequently, for the reinforced samples, the specific CB grades were added gradually. The mixing continued for approximately 2 h to achieve a uniform dispersion and breakdown of agglomerates. Finally, the curing system was incorporated, and mixing continued for an additional 15 min. For samples containing wax, the specific wax grade (1 phr) was added prior to the curing agents. To vulcanize the compounds, the samples were compression molded using a hydraulic hot press (Carver, USA) at 160°C for 10 min under 15 MPa pressure. Figure 1 illustrates the sample preparation and testing workflow, as well as the equipment and prepared elastomer specimens.

The curing system formulation was tabulated in Table 2. Upon these experiments, the effect of the types of EPDM, the ratios of carbon black (CB), and the types of waxes on the properties of elastomeric composites was tested.

2.3 | Mechanical Properties

To determine the tensile behavior of the specimens, an Instron 4201 universal testing machine (Instron, USA) was employed following the ASTM D 412 standard, type C. This standard specifies a grip separation speed of 500 mm/min. Likewise, the Shore A hardness of the vulcanized samples was measured according to ASTM D2240 using a Shore A Durometer (Bareiss, Germany). The test was carried out on the stacking of four sheets. The mechanical test results represent the average of five repeated specimens.

2.4 | Differential Scanning Calorimetry (DSC)

The glass transition and crystallization behaviors of the materials were studied using a DSC2500 (TA Instruments, USA) under a nitrogen atmosphere. Each sample of 10 ± 0.1 mg was cut from the vulcanized sheet and enclosed in a sealed aluminum pan. The samples were first heated at a heating rate of 10°C/min from 25°C to 180°C, maintained at this temperature for 0.5 min to eliminate any prior thermal history, and then cooled to −80°C at the rate of −10°C/min and reheated another time to 180°C at a heating rate of 10°C/min.

2.5 | Electrical Conductivity Test

The electrical conductivity of samples was measured using a broadband dielectric spectrometer (Novocontrol, Germany). Samples with an average thickness of 1 mm were sandwiched between two solid brass electrodes in a parallel-plate geometry (40 mm in diameter) while placed in a temperature-controlled chamber with a stability of 0.5°C. The complex permittivity ($\varepsilon^*(\omega)$) was measured as a function of frequency (ω) (in Hz), where:

$$\epsilon^* (\omega) = \epsilon' (\omega) - j\epsilon'' (\omega) \tag{1}$$

where $\varepsilon'(\omega)$ is the real part (dielectric constant) and $\varepsilon''(\omega)$ is the imaginary part (dielectric loss). The AC electrical conductivity $\sigma(\omega)$ was determined using the relation:

$$\sigma (\omega) = \omega\epsilon_0\epsilon'' (\omega) \tag{2}$$

where $\varepsilon_0 = 8.854 \times 10^{-12}$ F/m is the permittivity of free space. The DC conductivity (σ_{DC}) (in S/cm) was approximated using the conductivity value at the lowest measured frequency (0.1 Hz), when the conductivity reaches a plateau at low frequencies.

2.6 | Dynamic Mechanical Analysis (DMA) Test Method

The DMA test was performed on the samples to characterize their viscoelastic behaviors. The DMA 850 (TA Instruments, USA) was conducted in single-cantilever beam mode using a fixed frequency of 1 Hz and a displacement amplitude of 20 μm. The temperature was swept from −90 °C to 80 °C at a constant heating rate. The storage modulus (*E'*), loss modulus (*E''*), and loss factor (*tan (δ)*) were monitored to characterize the material's thermo-mechanical behavior over the entire temperature range.

2.7 | Swelling Test

The swelling tests are conducted on samples according to the ASTM D471 standard, with two repetitions for each formulation, to evaluate the cross-link density of the samples. Toluene is used as the swelling solvent. Initially, the initial weight of the samples (w_i) is measured. Then samples were immersed in toluene for 72 h at room temperature. After the swelling period, the samples were taken out, and any excess solvent was removed using filter paper. The weight of the swollen samples (w_s) was then measured. Finally, the samples are dried by oven drying at 70°C for 2 h to achieve the dry weight (w_d). To calculate the swelling ratio and insoluble fraction following equations were used:

$$\text{Swelling } (\%) = \frac{(w_s - w_i)}{w_i} \times 100 \tag{3}$$

$$\text{Insoluble fraction } (\%) = \frac{w_d}{w_i} \times 100 \tag{4}$$

where the w_i, w_s, and w_d are the weights of initial, swollen, and dried rubber (in g), respectively. The rubber's volume fraction (v_r) was determined using the following equation:

$$v_r = \frac{1}{1 + \frac{\rho_r}{\rho_t}\left(\frac{w_s - w_d}{w_d * (F_p)}\right)} \tag{5}$$

where ρ_r and ρ_t are the densities of the rubber and toluene, respectively. w_s and w_d are the weights of the swollen and the dried rubber samples. F_p is the fraction of the polymer in the system. Then, with v_r calculated above, the cross-link density of the samples (ρ_c) (in mol/cm^3) is calculated by using the Flory–Rehner equation:

$$\rho_c = -\frac{1}{2v_s} \times \frac{\ln(1 - v_r) + v_r + \chi v_r^{\,2}}{v_r^{\frac{1}{3}} - 0.5\, v_r} \tag{6}$$

In which v_s is the molar volume of the solvent, with a value of 106.36 cm^3/mol [21], and χ is the parameter of rubber-solvent interaction for EPDM and toluene, which is 0.49 [23].

3 | Results and Discussion

3.1 | Tensile Test

The tensile test curves for three types of unreinforced EPDM are shown in Figure 2a. To compare the three types of EPDM, they were vulcanized using the same curing formulation. Tensile test results showed that E47 exhibited the highest stress at break and elongation at break, followed by E65 and E45. This could be attributed to the higher crystallinity of E47, followed by E65, in comparison to E45. This is because EPDM composites with high ethylene content show superior tensile behavior owing to the orientation of crystalline phases under stress [17, 24, 25]. However, since the difference in ethylene content between the E45 and E65 is not significant, their overall behavior remained similar.

The tensile test curves and DSC curves for reinforced E47 and E45 samples are shown in Figure 2b,c. As observed, the elastomer composite based on E47 exhibited superior mechanical properties compared to E45. This could be related to the higher contents of ethylene groups in this EPDM, which promotes the formation of crystals. This crystal formation can be justified by the melting peak for EPDM. This allows to composite to be elongated more upon stretching during the tensile test and consequently results in higher tensile stress and elongation at break. It was also seen that the tensile strength of the reinforced samples was ten times greater than that of the unreinforced sample. For elongation at break, the increase was approximately twofold for E45 and about 1.5 times for E47 compared to their unfilled counterparts, respectively. The improvement of the mechanical properties upon the addition of CBs is due to their reinforcing effect on the system. The improvement of tensile stress and strain of the base polymer with the addition of 10–40wt.% [13], 20–60 phr [14], and 40–80 phr [16] of different types of CB was reported for EPDM [13, 14, 16], and with the addition of 5–60 phr of CB into styrene-butadiene rubber (SBR) [26].

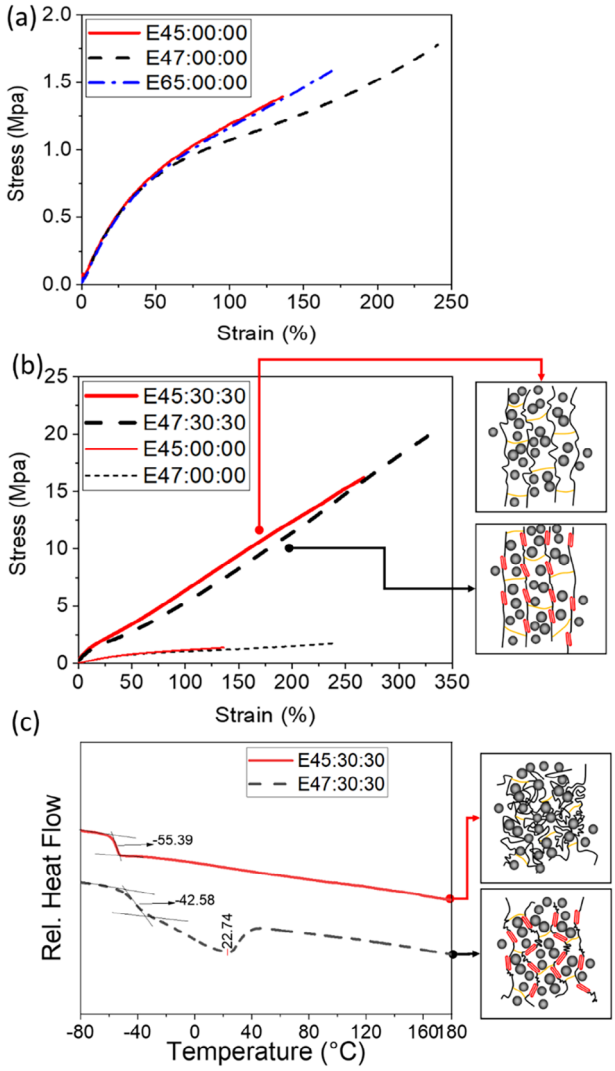

FIGURE 2 | Stress–strain curves of three types of (a) unreinforced EPDM, (b) reinforced EPDM, and (c) DSC tests of reinforced *EPDM*.

3.2 | Insoluble Fraction and Swelling Properties of Samples

Weight swelling and insoluble fraction of samples are shown in Figure 3. The insoluble fraction was identical for all formulations, indicating that the overall percentage of crosslinking is similar for all formulations. For the change in the contribution of CBs, the results revealed that by reducing the portion of CB550 in the system, the percentage of swelling increased. This can be attributed to the higher sulfur percentage in the CB, as it is mentioned in Table 1. The sulfur is available in the carbon black structure. However, not all these sulfurs are active or available at the surface, but they could increase the crosslink density and/or bound rubber in the vicinity of CB aggregates and/or agglomerations. Thus, it reduces the swelling percentage of the compound while having the same overall insoluble fraction. This means the type of CB can play an important role in polymer crosslinking. Therefore, having a dense crosslink density, the polymer could be less swollen with toluene. This was also reported for a peroxide-cured EPDM system in which, although the curing agent was peroxide, the sulfur available on the surface of carbon

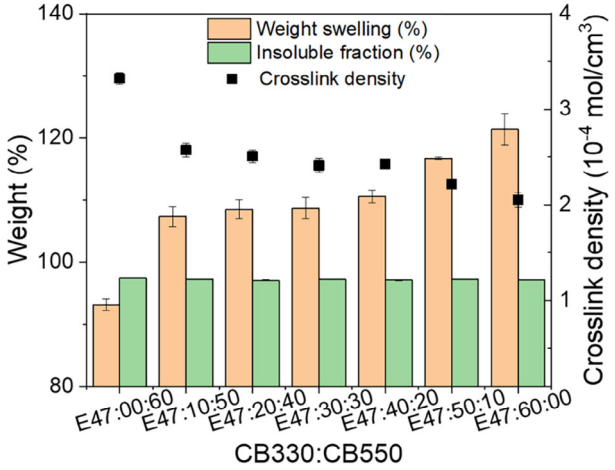

FIGURE 3 | Weight swelling, insoluble fraction, and crosslink density.

blacks intervened in the curing by increasing crosslink density [15].

3.3 | Tensile properties of Different Contributions of Carbon Black

The variation in stress, elongation at break, and modulus at 100% strain (100% modulus) with varying CB ratios is illustrated in Figure 4a. As the results of the tensile test reveal, both the elongation at break and the stress at break increased with increasing CB330 content. This enhancement in properties upon the substitution of CB550 with CB330 (at a constant total filler loading) is attributed to a reduced amount of sulfur, which otherwise increases the crosslink density and decreases the elongation at break [15], as well as the smaller structure size and higher surface area of the CB330 [27]. Consequently, the filler is less restricted by polymer crosslinks while simultaneously maintaining better interaction with the polymer. These factors facilitate the uniform movement of CB particles with the polymer chains during tension, thereby improving the matrix's ability to transfer force and enhancing the material's load-bearing capacity. In total, by substituting CB550 with CB330 in the set of samples tested, increases of approximately 40% and 56% were recorded for the stress and elongation at break, respectively. The highest values for stress and elongation at break were observed with 60 phr of CB330 (E47:60:00).

However, the 100% modulus exhibited a decreasing trend as the ratio of CB330 to CB550 increased. With a higher CB330 contribution, the system presents a less rigid barrier to deformation, likely due to the smaller amount of sulfur and finer structure of this carbon black. Since these particles generate a lower local crosslink density and possess a finer size, they interact more readily with the polymer matrix and deform with it. The total variation was about 20%, and the lowest 100% modulus was recorded for the compound with 60 phr of CB330 (E47:60:00).

This demonstrates that several formulations with different characteristics can be developed solely by changing the ratio of the carbon black. This flexibility is inportant, especially when the

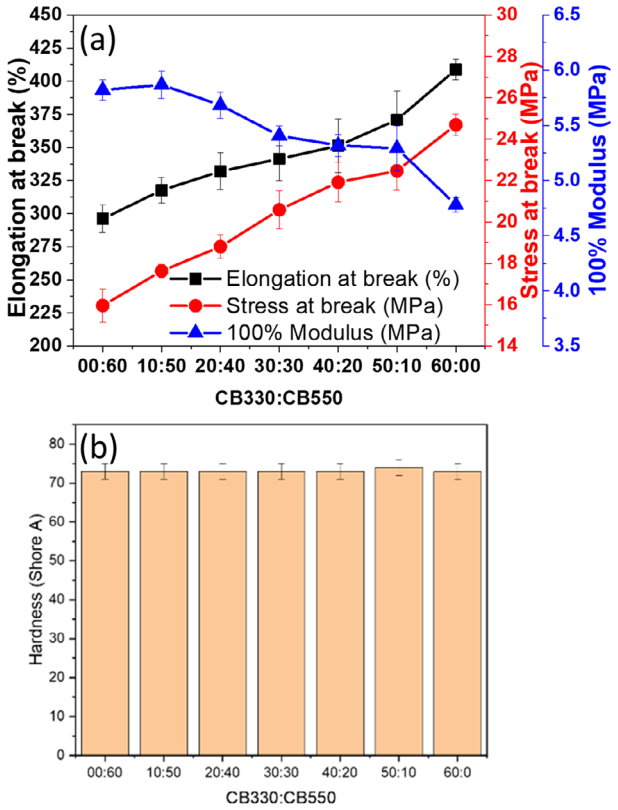

FIGURE 4 | The change in (a) tensile properties, stress, elongation at break, and 100% modulus with varying CB ratios, (b) hardness properties vs. the ratio of CB330:CB550.

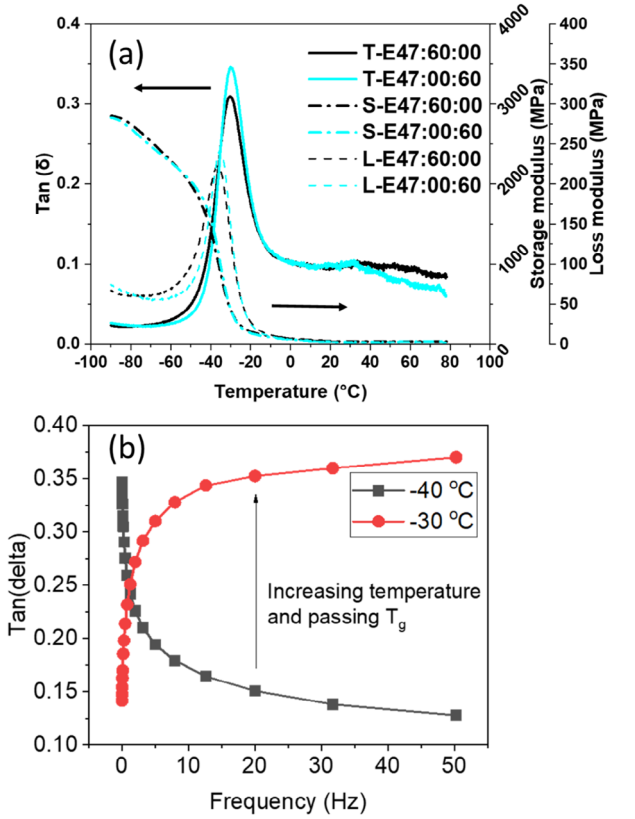

FIGURE 5 | The results of (a) the temperature sweep of the samples, and (b) the frequency sweep of the E47:30:30 sample.

overall properties are suitable for the application, yet specific adjustments are required to meet the precise values recommended by standards for overhead spacer dampers.

The hardness properties as a function of the ratio of CB330:CB550 are illustrated in Figure 4b. No significant changes were observed with variations in the ratio of the two types of carbon black. Since the total filler loading is the same in all cases, it can be inferred that hardness is independent of the structure and particle size of the two types of carbon black under study. This contrasts with the tensile properties, which strongly depend on the contribution of the two types of CB. Similar behaviors were reported for natural rubber compounds with the replacement of N220 with N550 [27], and also for natural rubber and acrylic rubber blends where the replacement of N220 with N330 did not alter the hardness [28]. This independence in hardness can be attributed to the static nature of the hardness test. As a result, the overall loading of carbon black in the system is more significant than the type of carbon black used or its interaction with the polymeric matrix. In addition, this implies that hardness depends more on the overall extent of cure (insoluble fraction) and not on the variations in crosslink density in the range studied.

3.4 | Results of the DMA Test

The results of the temperature sweep of samples are shown in Figure 5a. The DMA temperature sweep results for the storage modulus showed that as the temperature increased, the mobility of rubber segments gradually increased, leading to softening of the material and a progressive reduction in storage modulus [29]. The slightly higher storage modulus and higher loss modulus of the CB330-filled sample than those of the CB550-filled sample were seen at temperatures below −40°C. However, above −40°C, the loss modulus of the CB330-filled sample became lower than that of the CB550-filled sample. With the increase in temperature, the values of the two samples were the same. The change of In addition, the position of the *tan (δ)* peak did not change with the substitution of CB330 by CB550 in the samples, which means that the properties were dominated by the overall crosslinking ratio and not the crosslink density. However, the intensity of the *tan (δ)* increased with with substitution of CB330 by CB550. It means that CB550 has increased the capacity of the damping of the material. It could be related to the higher structure of this type of CB. However, for the samples containing CB330, it was seen lower intensity which can be related to the fine distribution of the CB330, which increases the rigidity of the system by reducing the motions of the polymer chains at that temperature.

The results of the frequency sweep of the E47:30:30 sample are displayed in Figure 5b. Furthermore, the results of *tan (δ)* before and after glass transition temperature (T_g) showed that before Tg, the highest damping is for the lowest frequency, and with increasing frequency, the value of *tan (δ)* reduced with increasing frequency which means the system responds like a rigid material. Meanwhile, with increasing temperature beyond the Tg, it is evident that *tan (δ)* increased with frequency, which means the damping of the sample increased.

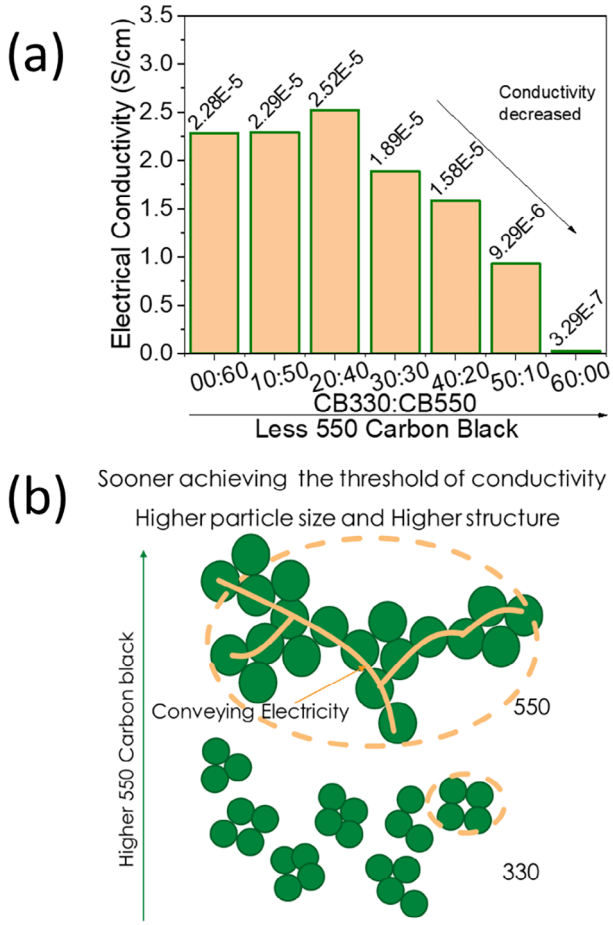

FIGURE 6 | (a) The results of the electrical conductivity of samples and (b) the mechanism of conductivity in the two types of carbon black.

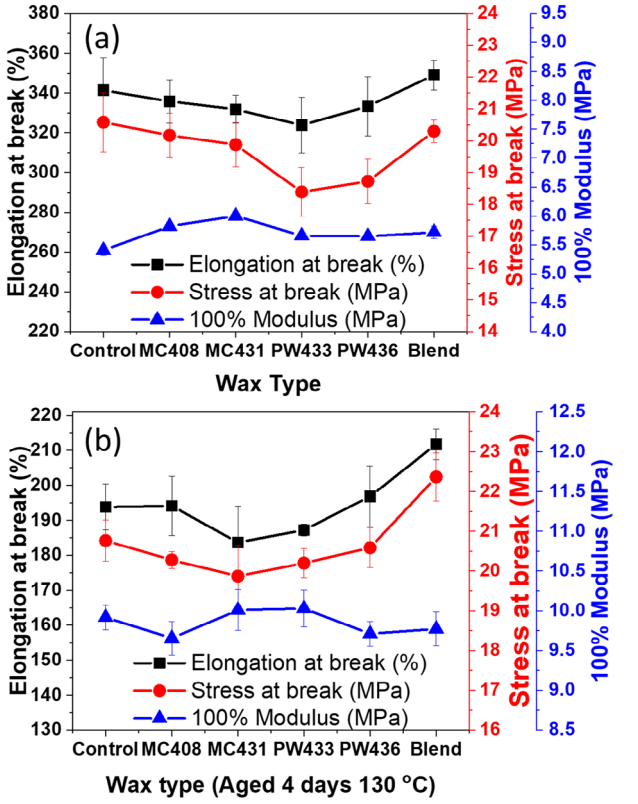

FIGURE 7 | The results of tensile tests of different wax-containing samples. (a) before and (b) after aging.

3.5 | Electrical Conductivity

In the electrical applications, semi-conductivity in the wire clamp rubber used on spacers is a key factor in preventing current formation on contaminated rubber surfaces caused by unbalanced voltages between sub-conductors [16]. Therefore, the effect of both the type and the different contributions of carbon blacks on the conductivity of EPDM rubber was examined [16, 30]. The results of the electrical conductivity tests are shown in Figure 6a.

Electrical percolation theory states that conductivity in polymer composites rises sharply once the filler content exceeds a critical threshold, where isolated particles begin forming continuous conductive networks [31]. Below this point, charge transport occurs mainly through tunneling or hopping, resulting in very low conductivity, while above it, the connected pathways allow much higher charge mobility [31, 32]. In our study, although the total filler loading was fixed at 60 phr, the percolation threshold was strongly influenced by the specific particle size, structure, and surface area of the carbon blacks used. The results revealed that as the proportion of CB550 decreased, electrical conductivity initially increased slightly before subsequently decreasing. Formulations containing 30 phr or more of CB550 exhibited the highest electrical conductivity. This behavior can be attributed to the larger particle size and higher structure of CB550, which enable it to form conductive agglomerations at lower loadings. This mechanism is illustrated in Figure 6b. Consequently, the percolation threshold is reached at a lower concentration with CB550 than with the finer CB330. These agglomerates facilitate electron transport by forming multiple pathways within the matrix, thereby reducing electrical resistivity. The observation of stable conductivity values suggests that the substitution of 10 phr of CB550 with CB330 did not significantly disrupt the network; effectively, the CB330 compensated for the reduction in CB550. The slight increase observed in sample E47:20:40 could be attributed to the fact that, despite the lower CB550 content, the CB330 particles likely bridged the gaps between CB550 aggregates, thereby enhancing conductivity. In many applications, maintaining a certain level of conductivity is necessary, even for insulators. High resistivity can lead to the accumulation of electrostatic charges, which may cause sparks or shocks.

3.6 | The Effects of Waxes on the Mechanical Properties

The results of tensile tests of wax-containing samples are shown in Figure 7a. The results showed that with the addition of 1 phr of each two microcrystalline waxes, the stress and elongation at break are reduced. However, the inverse trend was seen for 100% modulus, in which an increment was recorded with 1 phr of the microcrystalline waxes. This can be due to the fact that the waxes have a higher melting point in comparison to the EPDM used as the matrix. Therefore they increase the rigidity of the composite by impeding the replacement of chains, as it

could be seen as incresead 100% Modulus and reduced elongation and stress at break. This behavior is much more pronounced for MC431. It can be related to the fact that the melting temperature for this type is much higher means that it was much more rigid at ambient temperature and, as a result, less flexible in the tensile test. For the paraffin waxes, also same effect was recorded; however, the reduction in elongation at break and stress at break was higher, and the 100% modulus was lower than that of the microcrystalline one. It can be attributed to a less branched structure in comparison with that of microcrystalline, which makes it much more flexible with less entanglement in the system. Therefore, they can act as plasticizers and/or weak points with reducing the 100% modulus of the composite and causing premature fracture of the composite. It is much more pronounced for PW433, which has a lower melting temperature. A balance property was seen for the blend of microcrystalline and paraffin wax, in which elongation at break increased slightly in comparison to that of the control sample, and stress at break and 100% modulus were between the results obtained for the paraffin and microcrystalline waxes.

The results of the tensile properties of aged samples are shown in Figure 7b. As can be seen after thermo-oxidative aging, elongation at break for MC408 and P436 is near or less than the aged control sample, which means that they could marginally protect the material. However, the elongation at break for the sample containing a blend of paraffin wax and microcrystalline wax is higher, which is much more favorable for the application. Meanwhile, elongation at break of PW433 and MC431 was lower, which means they could not have a protective effect for the material. For the stress at break, for all the aged samples containing individual wax-filled samples, the stress at break is less than that of the aged unprotected ones. However, for the sample containing the blend of two waxes, the stress at break was recorded to have a higher value. It was seen that the 100% modulus had fluctuation with the different types of waxes, which means the protective effect of the type of waxes was negligible.

4 | Conclusion

This study shows that the choice of carbon black type, EPDM polymer, and waxes significantly affects the properties of elastomeric composites. Among the polymers tested, E47 exhibited the highest stress and elongation at break, likely due to its higher crystallinity compared to E65 and E45.

The addition of both types of CBs can improve the stress and elongation at the break of EPDM rubber. However, in hybrid CB-filled EPDMs, increasing the proportion of N330 carbon black improved stress and elongation at break but reduced electrical conductivity, likely due to its larger surface area and less sulfur in its structure, which interferes with crosslink formation. As swelling tests indicated a looser crosslinked structure in samples with more N330. Furthermore, substituting CB 550 with CB 330, while keeping the total loading constant at 60 phr, led to a dramatic 70-fold reduction in electrical conductivity, accompanied by notable enhancements in tensile strength (40%) and elongation at break (56%).

The addition of waxes influenced the mechanical properties differently. Microcrystalline waxes reduce the elongation and the stress at break while increasing the 100% modulus. Paraffin waxes acted the same way but with a much pronounced decrease in decreasing stress and elongation at break, however, with less 100% modulus. The blend of microcrystalline and paraffin wax provided a balanced effect, improving elongation with slightly lesser stress at break. Upon aging, Higher stress and elongation at break wax recorded in comparison to those of the aged control sample.

Overall, these findings suggest that adjusting the ratios of carbon black, choosing the appropriate EPDM type, and adding specific waxes can meaningfully alter the mechanical and electrical properties of elastomeric composites. For future work, it will be important to investigate the effects of other formulation ingredients on improving the mechanical, physical, and thermal-aging properties of the samples. In particular, examining different types of antioxidants and their combinations would be valuable, as these components can significantly influence the rubber crosslinking process.

Author Contributions

Conceptualization, M.T., M.E., and P.N.-T.; methodology, M.T.; preparation and analysis, M.T., M.E.; validation, M.T., M.E., and P.N.-T.; investigation, M.T.; resources, P.N.-T. and M.H.; data curation, M.T.; writing – original draft preparation, M.T.; writing – review and editing, M.T., M.E., M.H., and P.N.-T.; S.E.; E.D. All authors have read and agreed to the published version of the manuscript.

Acknowledgements

Special thanks to the technicians who have helped us complete this project.

Funding

This research was funded by the Natural Sciences and Engineering Research Council of Canada (NSERC), Prima-Quebec, Hydro-Québec, and Helix-Canada.

Conflicts of Interest

The authors declare no conflicts of interest.

Data Availability Statement

Data available on request, due to privacy/ethical restrictions.

References

1. D. Prasad, R. P. Singh, I. Khan, and S. Mukherjee, "Harmonic Dynamic Response Study of Overhead Transmission lines," in *Intelligent Data Mining and Analysis in Power and Energy Systems* (Wiley-IEEE Press, 2022), 257–280, https://doi.org/10.1002/9781119834052.

2. Y. D. Kubelwa, A. G. Swanson, D. G. Dorrell, and K. O. Papailiou, "A Comparative Study on High-Voltage Spacer-Damper Performance and Assessment: Theory, Experiments and Analysis," *SAIEE Africa Research Journal* 110, no. 3 (2019): 153–166, https://doi.org/10.23919/SAIEE.2019.8732787.

3. X. Fu, H.-N. Li, J.-X. Li, and P. Zhang, "A Pounding Spacer Damper and Its Application on Transmission Line Subjected to Fluctuating Wind

Load," *Structural Control and Health Monitoring* 24, no. 8 (2017): 1950, https://doi.org/10.1002/stc.1950.

4. P. V. Hung, H. Yamaguchi, M. Isozaki, and J. H. Gull, "Large Amplitude Vibrations of Long-span Transmission Lines With Bundled Conductors in Gusty Wind," *Journal of Wind Engineering and Industrial Aerodynamics* 126 (2014): 48–59, https://doi.org/10.1016/j.jweia.2014.01.002.

5. P. Van Dyke, U. Cosmai, and C. Freismuth, "Fittings," in *Overhead Lines. CIGRE Green Books*, ed. K. O. Papailiou (Springer, 2017), 417–558, https://doi.org/10.1007/978-3-319-31747-2.

6. Z. Zhao, B. Liu, S. Liu, D. Zhang, and R. Luo, "Design and Test of Quad-bundle Spacer Damper Based on a New Rubber Structure," *Shock and Vibration* 2023 (2023): 3828501, https://doi.org/10.1155/2023/3828501.

7. F. Zorić, S. Flegarić, G. Vasiljević, S. Bogdan, and Z. Kovačić, "Autonomous Installation of Electrical Spacers on Power Lines Using Magnetic Localization and Special End Effector," *Machines* 11 (2023): 510, https://doi.org/10.3390/machines11050510.

8. R. B. Simpson, *Rubber Basics* (Rapra Technology Limited, 2002), 77–89.

9. I. Surya, M. Muniyadi, and H. Ismail, "A Review on Clay-Reinforced Ethylene Propylene Diene Terpolymer Composites," *Polymer Composites* 42, no. 4 (2021): 1698–1711, https://doi.org/10.1002/pc.25956.

10. J. Song, K. Tian, L. Ma, W. Li, and S. Yao, "The Effect of Carbon Black Morphology to the Thermal Conductivity of Natural Rubber Composites," *International Journal of Heat and Mass Transfer* 137 (2019): 184–191, https://doi.org/10.1016/j.ijheatmasstransfer.2019.03.078.

11. M. Rahaman, "Superior Mechanical, Electrical, Dielectric, and EMI Shielding Properties of Ethylene Propylene Diene Monomer (EPDM) Based Carbon Black Composites," *RSC Advances* 13, no. 36 (2023): 25443–25458, https://doi.org/10.1039/d3ra04187e.

12. A. N. Uttaravalli, S. Dinda, V. R. Kakara, A. V. R. Rao, T. Daida, and B. R. Gidla, "Sustainable Use of Recycled Soot (carbon black) for the Cleaner Production of Value-added Products: A Compendium," *Chemical Engineering Journal Advances* 11 (2022): 100324, https://doi.org/10.1016/j.ceja.2022.100324.

13. J. Guo, P. Xu, J. Lv, et al., "Ageing Behaviour and Molecular/Network Structure Evolution of EPDM/Carbon Black Composites Under Compression and in Thermal-oxidative Environments," *Polymer Degradation and Stability* 214 (2023): 110417, https://doi.org/10.1016/j.polymdegradstab.2023.110417.

14. A. Shamsabadi, A. Farahani, M. M. Shirkavand, M.-J. Hafezi, and M. Tohidian, "Carbon Black/Ethylene Propylene Diene Monomer (EPDM) Rubber as Polymer Electrolyte Membrane Fuel Cell Gaskets: Mechanical and Chemical Assessment," *Iranian Polymer Journal* 33, no. 2 (2023): 169–183, https://doi.org/10.1007/s13726-023-01239-9.

15. Z. H. Li, J. Zhang, and S. J. Chen, "Effects of Carbon Blacks With Various Structures on Vulcanization and Reinforcement of Filled Ethylene-propylene-diene Rubber," *Express Polymer Letters* 2, no. 10 (2008): 695–704, https://doi.org/10.3144/expresspolymlett.2008.83.

16. Q. Wang, M. Yao, Y. Quan, and D. Zhuang, "Simultaneously Achieving Excellent Heat Aging Resistance and Grip Performance in Carbon Black/Glass Flake/EPDM Rubber Composite for Overhead Line Spacers," *Materials Today Communications* 39 (2024): 108878, https://doi.org/10.1016/j.mtcomm.2024.108878.

17. J. Tu, X. Shi, Y. Jing, et al., "Relationships of Tensile Strength With Crosslink Density for the High-Carbon Black-Filled EPDM Compounds With Various Softeners," *Polymer Engineering & Science* 61, no. 8 (2021): 2213–2221, https://doi.org/10.1002/pen.25750.

18. M. Tayefi, M. Eesaee, M. Hassanipour, S. Elkoun, E. David, and P. Nguyen-Tri, "Recent Progress in the Accelerated Aging and Lifetime Prediction of Elastomers: A Review," *Polymer Degradation and Stability* 214 (2023): 110379, https://doi.org/10.1016/j.polymdegradstab.2023.110379.

19. K. Bensalem, M. Eesaee, M. Hassanipour, et al., "Lifetime Estimation Models and Degradation Mechanisms of Elastomeric Materials: A Critical Review," *Polymer Degradation and Stability* 220 (2024): 110644, https://doi.org/10.1016/j.polymdegradstab.2023.110644.

20. I. Hamouda, M. Eesaee, and P. Nguyen-Tri, "Elastomer Service Life: The Role of Thermal and Mechanical Test Data in Predictive Analysis," in *Materials for Sustainable Environmental, Energy, and Bioresource Applications*, ed. P. Nguyen-Tri (Springer, 2024), 179–205, https://doi.org/10.1007/978-3-031-60255-9_13.

21. M. Tayefi, M. Eesaee, M. Hassanipour, S. Elkoun, E. David, and P. Nguyen-Tri, "Thermal Aging Behavior and Lifetime Prediction of Industrial Elastomeric Compounds Based on Styrene–butadiene Rubber," *Polymer Engineering & Science* 45 (2025): 3226–3246, https://doi.org/10.1002/pen.27210.

22. I. Hamouda, M. Tayefi, M. Eesaee, M. Hassanipour, and P. Nguyen-Tri, "Kinetic Analysis of Thermal Degradation of Styrene–Butadiene Rubber Compounds Under Different Aging Conditions," *Journal of Composites Science* 9, no. 8 (2025): 420, https://doi.org/10.3390/jcs9080420.

23. X. Zhang, J. Li, Z. Chen, C. Pang, S. He, and J. Lin, "Study on Thermal-oxidative Aging Properties of Ethylene-propylene-diene Monomer Composites Filled With Silica and Carbon Nanotubes," *Polymers* 14, no. 6 (2022): 1205, https://doi.org/10.3390/polym14061205.

24. P. S. Ravishankar, "Treatise on EPDM," *Rubber Chemistry and Technology* 85, no. 3 (2012): 327–349, https://doi.org/10.5254/rct.12.87993.

25. Y. Ma, Y. P. Wu, Y. Q. Wang, and L. Q. Zhang, "Structure and Properties of Organoclay/EPDM Nanocomposites: Influence of Ethylene Contents," *Journal of Applied Polymer Science* 99, no. 3 (2005): 914–919, https://doi.org/10.1002/app.22247.

26. Y. Merckel, J. Diani, M. Brieu, and J. Caillard, "Effects of the Amount of Fillers and of the Crosslink Density on the Mechanical Behavior of Carbon-Black Filled Styrene Butadiene Rubbers," *Journal of Applied Polymer Science* 129, no. 4 (2013): 2086–2091, https://doi.org/10.1002/app.38925.

27. R. Murniati, A. F. Gunawan, A. S. Hidayat, et al., "Enhancing Airless Tire Performance for Military Vehicles: Natural Rubber Compound With Carbon Black Fillers N220 and N550 With Dynamic Mechanical Analysis Approach," *Journal of Polymer Research* 31, no. 5 (2024): 137, https://doi.org/10.1007/s10965-024-03981-x.

28. J. Wootthikanokkhan and N. Rattanathamwat, "Distribution of Carbon Black in Natural Rubber/Acrylic Rubber Blends," *Journal of Applied Polymer Science* 102, no. 1 (2006): 248–256, https://doi.org/10.1002/app.23642.

29. J. Chen, M. Hu, Y. Li, R. Li, and L. Qing, "Significant Influence of Bound Rubber Thickness on the Rubber Reinforcement Effect," *Polymers* 15, no. 9 (2023): 2051, https://doi.org/10.3390/polym15092051.

30. Z. Li, B. Du, Y. Zhao, and T. Han, "Semi-Conductive Polymer Composites for Power Cables," *Polymer Composites for Electrical Engineering*, eds. X. Huang and T. Tanaka (Wiley-IEEE Press, 2021), 153–178, https://doi.org/10.1002/9781119719687.

31. S. Huang, Z. Liu, C. Yin, et al., "Dynamic Electrical and Rheological Percolation in Isotactic Poly(propylene)/Carbon Black Composites," *Macromolecular Materials and Engineering* 297, no. 1 (2011): 51–59, https://doi.org/10.1002/mame.201100150.

32. L. S. Vieira, E. G. R. dos Anjos, G. E. A. Verginio, et al., "A Review Concerning the Main Factors That Interfere in the Electrical Percolation Threshold Content of Polymeric Antistatic Packaging With Carbon Fillers as Antistatic Agent," *Nano Select* 3, no. 2 (2021): 248–260, https://doi.org/10.1002/nano.202100073.